Detection of Membrane Packing Defects by Time-Resolved Fluorescence Depolarization

Sun-Yung Chen and Kwan Hon Cheng
Department of Physics, Texas Tech University, Lubbock, Texas 79409-1051 USA

ABSTRACT Packing defects in lipid bilayer play a significant role in the biological activities of cell membranes. Time-resolved fluorescence depolarization has been used to detect and characterize the onset of packing defects in binary mixtures of dilinoleoylphosphatidylethanolamine/1-palmitoyl-2-oleoylphosphatidylcholine (PE/PC). These PE/PC mixtures exhibit mesoscopic packing defect state (D), as well as one-dimensional lamellar liquid crystalline (L_α) and two-dimensional inverted hexagonal (H_{II}) ordered phases. Based on previous electron microscopic investigations, this D state is characterized by the presence of interlamellar attachments and precursors of H_{II} phase between the lipid layers. Using a rotational diffusion model for rod-shaped fluorophore in a curved matrix, rotational dynamics parameters, second rank order parameter, localized wobbling diffusion, and curvature-dependent rotational diffusion constants of dipyenylhexatriene (DPH)-labeled PC (DPH-PC) in the host PE/PC matrix were recovered from the measured fluorescence depolarization decays of DPH fluorescence. At ~60% PE, abrupt increases in these rotational dynamics parameters were observed, reflecting the onset of packing defects in the host PE/PC matrix. We have demonstrated that rotational dynamics parameters are very sensitive in detecting the onset of curvature-associated packing defects in lipid membranes. In addition, the presence of the D state can be characterized by the enhanced wobbling diffusional motion and order packing of lipid molecules, and by the presence of localized curvatures in the lipid layers.

INTRODUCTION

Besides ordered phases (Gruner et al., 1985) of well-defined geometries, several lipid mixtures exhibit a mesoscopic defect (D) state with no long-range translational order (Boni and Hui, 1983; Cheng et al., 1994). This mesoscopic D state is usually composed of interlamellar packing defects, disordered amorphous aggregates, and precursors of nonbilayer phases among the lipid layers. The existence as well as the onset of this D state are believed to play an important role in triggering several lipid-specific properties, such as membrane fusion (Burgess et al., 1992) and release of liposomal drugs (Litzinger and Huang, 1992). At present, knowledge of the detection and characterization of the onset of the D state in pure and biological membranes is still incomplete (Epand, 1995).

Conventional x-ray diffraction is a valuable tool in revealing structures of order phases (Gruner et al., 1985). However, because of the lack of long-range translational order (Boni and Hui, 1983), the onset of the mesoscopic state can only be detected by other spectroscopic measurements, such as NMR (Boni and Hui, 1983), fluorescence (Cheng et al., 1994; Epand, 1995), and infrared (Cheng, 1994). It is believed that the appearance of localized curvature in the lipid layers is an important signature of the D state (Boni and Hui, 1983, and references therein). Our previous fluorescence depolarization studies (Cheng, 1989; Chen et al., 1990) have established that the rotational dynamics behavior of rod-shaped fluorophore is very sensitive to changes in the curvature of the membranes due to the first-order transition of lamellar-to-inverted hexagonal phases. In this study, a time-resolved fluorescence depolarization technique (Gratton et al., 1984; Cheng, 1989; Chen et al., 1992) was employed to test an important hypothesis. The hypothesis is that this time-resolved fluorescence depolarization technique is also capable of detecting and characterizing the onset of the curvature-related D state in membranes. Here a biologically relevant and well-defined binary lipid mixture system, phosphatidylethanolamine/phosphatidylcholine (PE/PC), was selected. A fluorescent lipid probe, diphenylhexatriene (DPH) chain-labeled PC (DPH-PC) (Cheng, 1989), was used to investigate the rotational diffusion and conformational order of the host PE/PC mixtures, which exhibit the mesoscopic D state, as well as one-dimensional lamellar liquid crystalline (L_α) and two-dimensional inverted hexagonal (H_{II}) ordered phases. The rotational diffusion model for rod-shaped fluorophore in curved matrix has been introduced and discussed in great detail in our previous studies of ordered phases (van der Meer et al., 1990; Chen et al., 1990, 1992). A very brief outline of this model is presented here.

MATERIALS AND METHODS

Sample preparations and structural morphologies of lipid/water mixtures

Dilinoleoyl PE (DLPE) and 1-palmitoyl-2-oleoyl PC (POPC) in chloroform were purchased from Avanti Polar Lipids (Birmingham, AL) and

Received for publication 30 January 1996 and in final form 25 April 1996.

Address reprint requests to Dr. Kwan-Hon Cheng, Department of Physics, Texas Tech University, Biophysics Laboratory, Box 41051, Lubbock, TX 79409-1051. Tel.: 806-742-2992; Fax: 806-742-1182; E-mail: vckhc@ttacs.ttu.edu.

Dr. Chen's present address is Department of Physics, Western Kentucky University, Bowling Green, KY 42101.

0006-3495/96/08/878/07 $2.00

used without further purification. DLPE is a lipid with two unsaturated acyl chains of 18 carbons, and POPC has one 16-carbon saturated and one 18-carbon unsaturated chain. At 23°C, fully hydrated DLPE suspensions form the H_{II} phase, whereas POPC suspensions form the L_α phase (Boni and Hui, 1983; and references therein). In the H_{II} phase, lipids form long, cylindrical monolayer tubes, with their polar headgroups facing the long water core (water-in-oil). On the other hand, in the L_α phase, lipids arrange in bilayer lamella in tail-to-tail orientation, with water in the space between adjacent planar surfaces of lipid polar headgroups. Based on previous combined electron microscopy and NMR investigations at 23°C (Boni and Hui, 1983), DLPE/POPC mixtures are in the L_α phase for DLPE $\leq$ 50%. The mesoscopic D state, in the form of interlamellar attachments and precursors of the H_{II} phase (or collectively known as packing defects), is found starting at ~80% DLPE. Finally, the H_{II} phase prevails for DLPE $\geq$ 95%.

Fluorescent lipid, 1-palmitoyl-2-((2-(4-(6-phenyl-*trans*-1,3,5-hexatrienyl)phenyl)ethyl)carbonyl)-3-*sn*-PC (DPH-PC), was obtained from Molecular Probes (Eugene, OR). This DPH-PC consists of a 16-carbon saturated fatty acyl chain attached to the *sn*-1 position of the glycerol backbone. A rigid rod-shaped diphenylhexatriene (DPH) is attached to the *sn*-2 position of the glycerol backbone via a short propanoyl chain. DPH-PC was used for fluorescence depolarization measurements. Another fluorescent lipid, 1-palmitoyl-2-(10-(1-pyrenyl)decanoyl)-PC (Py_rPC), was also obtained from Molecular Probes. Py_rPC consists of one 16-carbon saturated chain at the *sn*-1 position, and a 10-carbon saturated chain is at the *sn*-2 position, with a planar pyrene molecule attached to its methyl end. This Py_rPC was used for lateral diffusion measurements.

Fluorescent probe and PE/PC were mixed in chloroform. The molar ratio of DPH-PC to host PE/PC lipids was 1/1000. For Py_rPC, two different molar ratios, 5/1000 and 2/100, were used. Each probe/lipid mixture was dried under a stream of nitrogen in a clean pyrex tube and kept in a vacuum for at least 4 h to remove the residual organic solvent. The thin film formed on the tube was then hydrated with an aqueous buffer (100 mM NaCl, 10 mM *N*-tris[hydroxymethyl]methyl-2-aminoethanesulfonic acid and 2 mM EDTA, pH = 7.4) at 4°C. The suspension was vortexed vigorously and placed under mild sonication in a bath sonicator for a few seconds. The sonication facilitated dispersion of the lipids, particularly the poorly hydrated PEs, into suspensions. The mixture was then incubated overnight at 4°C in the dark to ensure proper hydration. Upon diluting to 0.1 mg/ml, the sample was then placed in a 10-mm quartz curvette for fluorescence measurements.

Time-resolved fluorescence lifetime and depolarization measurements

All time-resolved fluorescence measurements were performed on a frequency-domain cross-correlation fluorometer (ISS Inc., Champaign, IL), using a Liconix 4240NB cw He-Cd laser (Santa Clara, CA) with an output of 17 mW at 325 nm as the excitation source. The operational principle of this fluorometer has been described in detail elsewhere (Gratton et al., 1984; Lakowicz and Malieval, 1985).

The fluorescence lifetime of DPH-PC was measured by using a nonfluorescent glycogen solution as a reference. Because the light exiting from the pockels cell (electrooptical device) is vertically polarized, a polarizer with its polarization axis set at 35° with respect to the vertical was placed in the excitation beam to eliminate the contribution of the rotational diffusion effect of the sample to the measurements (Spencer and Weber, 1970; Cheng, 1989). A low-wavelength cutoff filter at 350 nm was used to remove the excitation light from the fluorescence signal. Both the phase delay ($\delta_F - \delta_S$) and modulation ratio (M_F/M_S) were measured at different modulation frequencies ($\omega/2\pi$) ranging from 1 to 300 MHz. Here δ_F and δ_S represent the phase delay of the emission signal from the fluorescent sample and that from the reference sample, respectively, with respect to the excitation light, and M_F and M_S represent the intensity modulation values of the fluorescent samples and that of the reference, respectively. It has been shown that $\delta_F - \delta_S$ and M_F/M_S correspond to the phase angle and absolute magnitude of a complex demodulation factor $m(\omega)$, which is proportional to the Fourier transform of the delta-response fluorescence intensity decay function $I(t)$ of the sample in the time space (Sugar, 1991).

The fluorescence lifetime of Py_rPC was also measured using the above frequency-domain technique. Here a monochrometer, instead of a cutoff filter, was used to select the monomer fluorescence intensity of conjugated pyrene at 392 nm. For the samples with a 5/1000 molar ratio of Py_rPC/lipid, only monomer fluorescence was detected, whereas for the 2/100 molar ratio samples, both monomer and excimer (located at 475 nm) fluorescence signals were found. The excimer fluorescence is due to the collision of a ground-state pyrene of Py_rPC with an excited pyrene of another Py_rPC (Galla et al., 1979; Sugar, 1991).

For the fluorescence depolarization measurements, both excitation and emission polarizers were used. The vertical direction refers to the initial excitation polarization of the laser. Differential polarized phase angle ($\delta_\perp - \delta_\parallel$) and polarized modulation amplitude ratio ($M_\parallel/M_\perp$) were measured at different modulation frequencies (1–300 MHz). The subscripts $\perp$ and $\parallel$ refer to the directions of the polarization axis of the emission polarizer that are perpendicular and parallel to the vertical axis, respectively. It has been shown that (Gratton et al., 1984)

$$(\delta_\perp - \delta_\parallel) = \tan^{-1}[(D_\parallel N_\perp - D_\perp N_\parallel)/(N_\parallel N_\perp + D_\parallel D_\perp)] \quad (1)$$

and

$$(M_\parallel/M_\perp) = [(N_\parallel 2 + D_\parallel^2)/(N_\perp^2 + D_\perp^2)]^{1/2}, \quad (2)$$

where N_i and D_i are the sine and cosine transforms of the delta-response polarization decay function $I_i(t)$ decay along the direction of $i = \perp$ or $\parallel$, respectively. The above equations provide the mathematical conversion or equivalence of the time-domain polarization data [$I_i(t)$] and the frequency-domain polarization data [$(\delta_\perp - \delta_\parallel)$ and $(M_\parallel/M_\perp)$].

Rotational diffusion model for rod-shaped fluorophore in curved matrix and fluorescence data analysis

We assume that the lateral diffusion of the rod-shaped (or cylindrical) DPH-PC around a curved layer, the wobbling diffusion of the whole DPH-PC molecule with respect to the normal of the membranes (local director), and the orientational distribution of the long DPH-PC axis with respect to the local director are the only major factors contributing to the fluorescence depolarization of DPH-PC. The justifications of the above assumptions have been discussed in detail elsewhere (Cheng, 1989; van der Meer et al., 1990). The anisotropy decay $r(t)$ of DPH-PC in a lipid layer can be written as

$$\begin{aligned} r(t) &= [I_\parallel(t) - I_\perp(t)]/[I_\parallel(t) + 2I_\perp(t)] \\ &= r_o\, Q_W\, Q_C, \end{aligned} \quad (3)$$

where r_o anisotropy is the anisotropy of the fluorophore at time 0, and Q_W and Q_C are the time-dependent depolarization factors due to wobbling and curvature-associated rotational diffusion of the fluorophore. It has been shown (van der Meer et al., 1990) that Q_W can be expressed as

$$Q_W = [\langle P_2\rangle^2 + (1 - \langle P_2\rangle^2)\exp[-6D_W t/(1 - \langle P_2\rangle^2)]. \quad (4)$$

The other factor Q_C in Eq. 3 can be written as (van der Meer et al., 1990; Chen et al., 1992)

$$Q_C = 0.25 + 0.75\exp(-4\,D_H T), \quad (5)$$

where

$$D_H = D_L/R^2. \quad (6)$$

The above Q_C is for a lipid layer exhibiting a cylindrically interfacial curvature. Here D_H represents the rotational diffusion coefficient of the

fluorophore around a cylindrical curvature of radius of curvature R, and D_L is the lateral diffusion constant of the probe molecule (Chen et al., 1992).

Equation 3 is known as the WOBHOP rotational diffusion model (van der Meer et al., 1990). Upon expanding the Q_w and Q_c, it is easy to see that $r(t)$ contains three exponential decay functions and one constant term. It is important to mention that D_H becomes zero for a planar lipid layer. This is because R approaches infinity for a planar surface (see Eq. 6). In that case, Q_C becomes 1. Therefore, $r(t)$ becomes identical to Q_w, which contains a single exponential decay function and one constant term (see Eq. 4). This simple $r(t)$ function is also called the one-exponential model (Chen et al., 1990). It is important to mention that Eq. 3 can be applied to both planar and curved lipid matrixes, and that D_H is the only rotational parameter that is directly associated with the local curvature of the lipid layer. From the measured frequency-domain polarization data, r_o, $\langle P_2 \rangle$, D_w, and D_H can be recovered using a nonlinear least-squares analysis procedure based on Eqs. 1–5 (Chen et al., 1990). The value of the square of the order parameter, i.e., $\langle P_2 \rangle^2$, is associated with the fluorescence anisotropy at a sufficiently long time, i.e., r_∞, and does not require any explicit assumptions of the form and parity of the ordering potential for the orientational dynamics of the probe in the membranes (van der Meer et al., 1990).

Lateral diffusion constant determination

The lateral diffusion coefficient D_L of the lipids can be estimated from the fluorescence lifetimes of Py_rPC by using a first-order classical random walk model (Galla et al., 1979; Chen et al., 1992, and references therein), i.e.,

$$D_L = 2/(\pi X_{py}) \ln(2/X_{py}) L^2 (\tau^{-1} - \tau_o^{-1})/4, \qquad (7)$$

where L (~8 Å) is the estimated length of one diffusion jump of pyrene molecule (Galla et al., 1979), X_{py} is the pyrene/lipid molar ratio, and τ and τ_o are the fluorescence decay lifetimes of monopyrene labeled lipids at high (2/100) and low (5/1000) probe/lipid molar ratios, respectively.

RESULTS

Fluorescence lifetimes of DPH-PC in DLPE/POPC binary lipid mixtures were measured as a function of DLPE% at room temperature (23°C); results are shown in Fig. 1. By using a single-exponential fit, the fluorescence lifetimes of DPH-PC were found to be around 6.3 ns and independent of DLPE%. A better fit was obtained by using a double-exponential decay function, as judged by the observation that the reduced χ^2 value of the double-exponential fit was smaller than that of the single-exponential fit. In this case, a major lifetime component of ~6 ns and a shorter lifetime component (1–2 ns) with an intensity fraction less than 0.04 were found. Again these two lifetime components and intensity fractions were independent of DLPE%. The extra short lifetime component is attributed to the minor but unavoidable degraded product of the fluorescent probe during the sample preparation (Parente and Lentz, 1985; Cheng, 1989). Based on the measured lifetime values and the amphiphilic characteristic of DPH-PC, it is believed that the site-selective DPH is located in the hydrocarbon region of the lipid layers and independent of the composition of the host lipid matrix (Parente and Lentz, 1985).

Fluorescence lifetimes of Py_rPC, τ, and τ_o for probe/lipid molar ratios of 2/100 and 5/1000, respectively, in DLPE/POPC at 23°C were also measured. From Eq. 7, the lateral diffusion coefficients D_L of lipids as a function of DLPE% were estimated from these lifetime values; results are shown in Fig. 2. D_L remained constant at around 5.5 cm^2/s as DLPE% was varied from 0% to 70%. As DLPE% increased from 70% to 90%, a peak at 80% DLPE with a D_L value of 7.5 cm^2/s was observed. As DLPE% increased further to 100% (H_{II}), D_L became constant again at around 5.0 cm^2/s.

Using the rotational diffusion model as described in Materials and Methods, various rotational dynamics parameters, r_o, $\langle P_2 \rangle$, D_W, and D_H, of DPH-PC, were recovered from the frequency-domain fluorescence depolarization measurements of DPH fluorescence in DLPE/POPC. Data fittings using one-exponential (D_H confined to zero) and WOBHOP

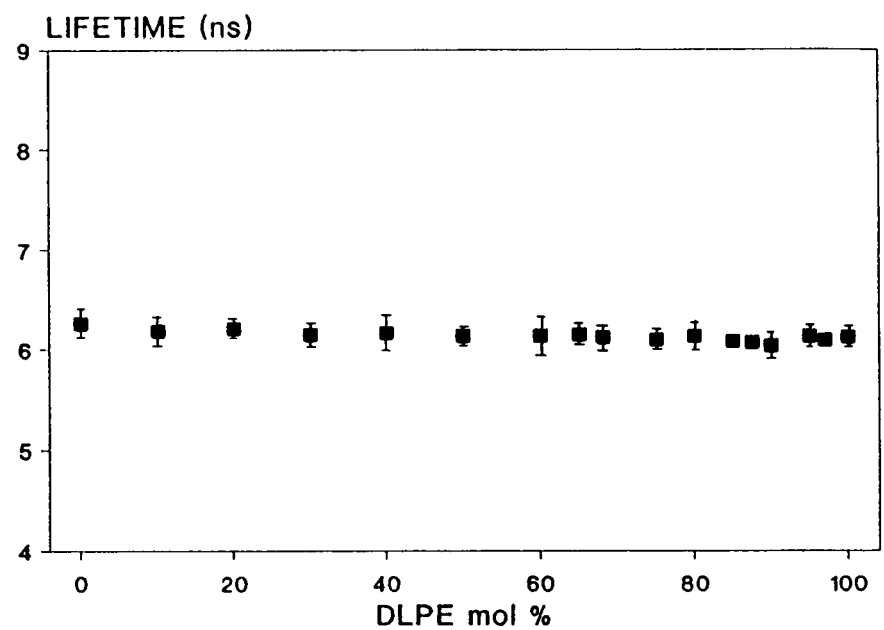

FIGURE 1 Fluorescence lifetime of DPH-PC in DLPE/POPC mixtures as a function of DLPE% at 23°C. Bars indicate confidence limits of the calculated parameters.

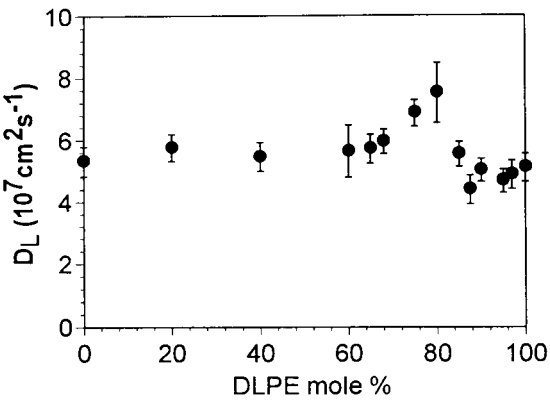

FIGURE 2 Lateral diffusion coefficient D_L of Py_rPC in DLPE/POPC mixtures as a function of DLPE% at 23°C. Bars indicate confidence limits of the calculated parameters.

(D_H not confined) models were performed. Table 1 shows some fitting results at three representative DLPE contents, 0%, 80%, and 97%. For DLPE < 60%, the values of the recovered parameters, r_o and $\langle P_2 \rangle$, obtained from either model were very similar. In addition, the parameters D_H obtained from the WOBHOP model were essentially zero. Importantly, within this DLPE% range, the reduced χ^2 from both models were very similar. For example, at 0% DLPE, as shown in Table 1, similar recovered values of 0.28 and 0.70 for r_o and $\langle P_2 \rangle$ were obtained from the two models. Furthermore, D_H was found to be 0.06 ± 0.20, i.e., practically zero, and the χ^2 value of 1.6 was found for both models. In contrast, for DLPE > 60%, $\langle P_2 \rangle$ and D_W obtained by the WOBHOP model started to deviate from those by the one-exponential model. Moreover, a significant improvement in the reduced χ^2 from the WOBHOP model over those from the one-exponential model was found. For example, at 80% and 97% DLPE% as shown in Table 1, χ^2 values of 2.9 and 2.1, respectively, were found for the one-exponential model, whereas considerably lower χ^2 values of 2.0 (80% DLPE) and 1.3 (97% DLPE) were obtained from the WOBHOP model. These results indicate that the WOBHOP model, which includes the curvature-associated D_H term, provides a statistically better description of the rotational dynamics of DPH-PC in the PE/PC membranes than does the one-exponential model with DLPE > 60%, whereas the one-exponential model with $D_H = 0$ is sufficient to describe the rotational behavior of DPH-PC in the PE/PC membranes with DLPE < 60%.

The initial anisotropy r_o and order parameter $\langle P_2 \rangle$ of DPH-PC in DLPE/POPC recovered from the WOBHOP model as a function of DLPE% at 23°C are shown in Fig. 3. For DLPE < 65%, $\langle P_2 \rangle$ was essentially constant at around 0.7. A noticeable and progressive increase in $\langle P_2 \rangle$ was observed as the DLPE content was increased from 60% to 85% DLPE. Thereafter the order parameter remained high at around 0.8 as the DLPE content was further increased to 100%. For r_o, no significant change was found at all DLPE contents.

The two rotational diffusion constants, D_W and D_H, of DPH-PC in DLPE/POPC recovered from the WOBHOP model as a function of DLPE% at 23°C are shown in Fig. 4. The behavior of D_W was very similar to that of D_L. Here D_W increased slightly from 2.4 to 2.8 × 10^7 s^{-1} as DLPE% was varied from 0% to 65%. In the range of 65–90% DLPE, a prominent peak with D_W around 3.8 × 10^7 s^{-1} was found at 80% DLPE. As DLPE% increased further to 100%, D_W again remained constant at around 3.0 × 10^7 s^{-1}. On the other hand, the behavior of D_H was similar to that of the order parameter. Here the curvature-dependent D_H remained essentially zero for DLPE < 65%, but increased steadily to around 2.0 × 10^7 s^{-1} as DLPE increased from 65% to 85%. Thereafter, D_H reached a plateau as the DLPE increased further to 100%.

The values of R, defined as the estimated radii of curvature of the lipid/water interface, were determined from the values of D_L and D_H using Eq. 6; the results are shown in Fig. 5. Large uncertainties in R within the range of 0–60% were due to the near-zero behavior of D_H as shown in Fig. 4 and Table 1. Here R was around 30 Å for DLPE between 65% and 80%. It dropped to around 20 Å at 90% and remained constant as DLPE increased further to 100%.

DISCUSSION

Time-resolved fluorescence depolarization has been used to detect and characterize the onset of packing defects in DLPE/POPC mixtures. Previous studies (Boni and Hui, 1983) based on ^{31}P NMR, x-ray diffraction, and electron microscopy on the same lipid system, revealed the existence of three zones, L_α phases (0–75% DLPE), "intermediate"

TABLE 1 Recovered rotational dynamics parameters based on the one-exponential and WOBHOP models

Models	Samples (% PE)	r_o	D_w (10^7 s^{-1})	D_H (10^7 s^{-1})	$\langle P_2 \rangle$	χ^2	R (Å)
One-exponential	0	0.28 ± 0.03	2.68 ± 0.06	—	0.70 ± 0.02	1.6	—
	80	0.25 ± 0.01	3.60 ± 0.06	—	0.73 ± 0.01	2.9	—
	97	0.26 ± 0.03	3.00 ± 0.03	—	0.65 ± 0.03	2.1	—
WOBHOP	0	0.28 ± 0.02	2.40 ± 0.16	0.06 ± 0.20	0.69 ± 0.01	1.6	94 (43, ∞)
	80	0.25 ± 0.03	3.68 ± 0.26	0.75 ± 0.21	0.76 ± 0.04	2.0	32 (26, 40)
	97	0.26 ± 0.04	2.85 ± 0.31	1.65 ± 0.36	0.83 ± 0.03	1.3	18 (15, 20)

The uncertainties of the recovered parameters and reduced χ^2 are also shown. Values between parentheses represent the upper and lower limits of the estimated radius of curvature calculated from the recovered D_H and D_L parameters (see Materials and Methods).

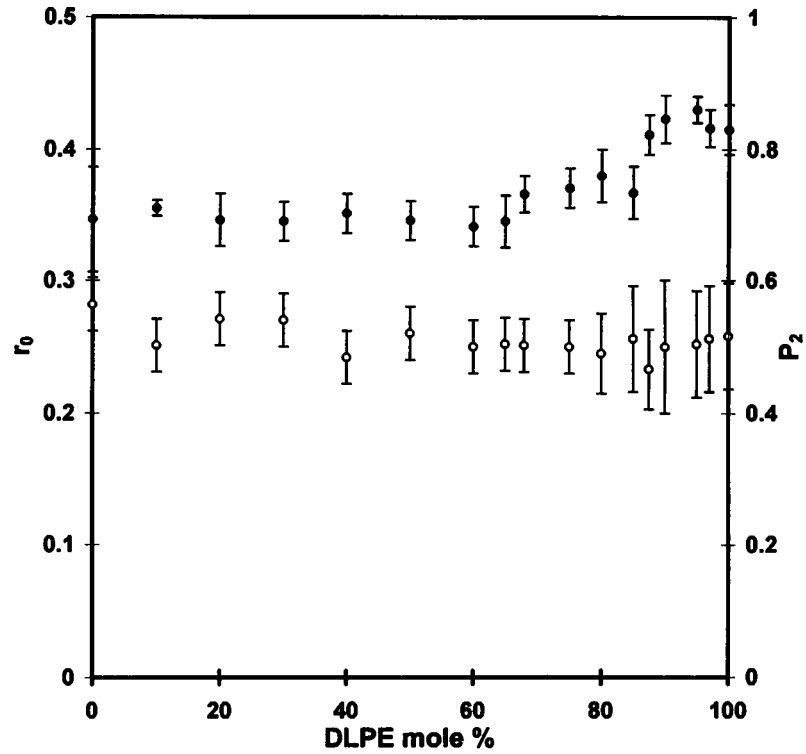

FIGURE 3 Initial anisotropy r_o (○) and local order parameter $\langle P_2 \rangle$ (●) of DPH-PC in DLPE/POPC mixtures based on the WOBHOP model as a function of DLPE% mixtures at 23°C. Bars indicate confidence limits of the recovered parameters.

state (75–90% DLPE), and H_{II} (95–100%) phases. The definition of "intermediate" state used in those previous studies is equivalent to the mesoscopic D state in this fluorescence study.

Time-resolved fluorescence has been used extensively to investigate rotational dynamics of fluorophores in protein and bilayer membranes (Ameloot et al., 1984; Deinum et al., 1988; Cheng and Lepock, 1992; van der Sijs et al., 1993; Muller et al., 1994; Thevenin et al., 1994). Recently we

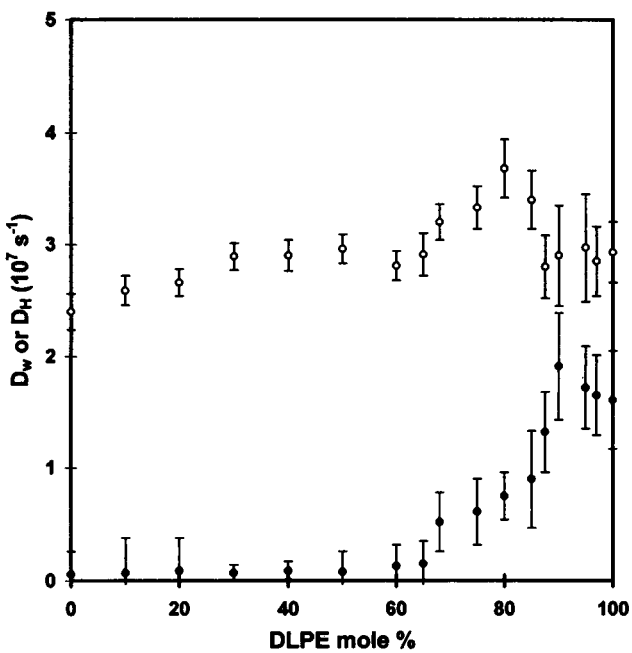

FIGURE 4 Wobbling diffusion constant D_W (○) and curvature-associated rotational diffusion constant D_H (●) of DPH-PC in DLPE/POPC mixtures based on the WOBHOP model as a function of DLPE% at 23°C. Bars indicate confidence limits of the calculated parameters.

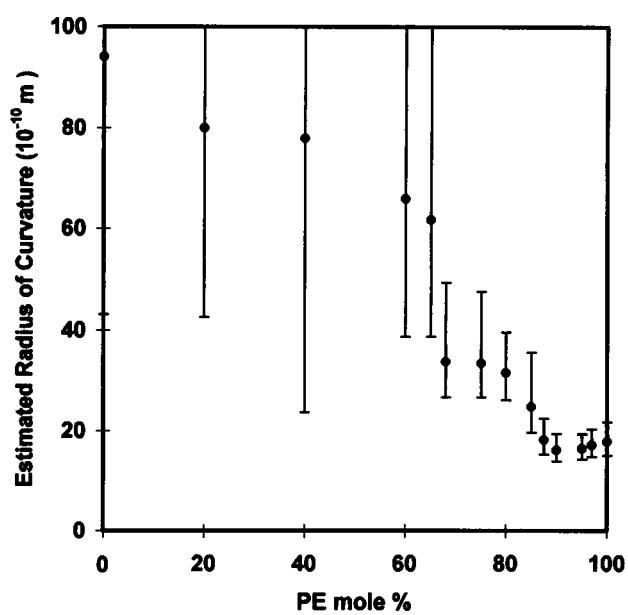

FIGURE 5 Estimated radius of curvature R of DLPE/POPC lipid layers in DLPE/POPC mixtures based on the measured D_H of DPH-PC and D_L of PyrPC in the same mixtures at 23°C. Bars indicate confidence limits of the calculated parameters.

have shown that this technique can also be used to characterize the molecular dynamics of nonbilayer ordered phases with cylindrical curvatures (Cheng, 1989; Chen et al., 1990, 1992) by including a curvature-dependent depolarization factor Q_C in the anisotropy decay equation originally used in a planar bilayer (van der Meer et al., 1990). In those studies, we have shown that the molecular dynamics parameters, both structural (order parameters) and rotational (wobbling and curvature-associated diffusion), of rod-shaped fluorophore are very sensitive to the existence of cylindrical curvature in membranes. The purpose of this study was to determine whether this nanosecond fluorescence technique can also be employed to detect and characterize the mesoscopic packing defect state, which has no long-range translational order but involves changes in curvatures.

The values of D_W of DPH-PC, as well as D_L of Py_rPC, increase significantly at around 60–70% DLPE and reach a peak at 80%. These observations suggest that the local wobbling diffusion of DPH in DPH-PC and translational diffusion motion of Py_rPC increase as the lipids enter the "intermediate" state from the L_α phase. The results indicate that both local rotational and translational mobilities of the DPH-PC molecules are responding to the presence of a intermediate state in the host matrix.

The order parameter $\langle P_2 \rangle$ also starts to increase at around 60–70% DLPE and to stay high as the lipids finally reach the H_{II} phase at the predicted 95–100% DLPE. This indicates that the packing constraint of the acyl chains increases as the lipids approach the "intermediate" state and remains high in the H_{II} phase. This enhancement in the order packing agrees with our previous fluorescence depolarization studies of temperature- and lipid composition-dependent L_α-to-H_{II} transition of single and binary lipid mixtures (Cheng, 1989; Chen et al., 1990, 1992). The important finding here is that the increase occurs as the lipids enter the "intermediate" or D state around 60–70% DLPE, well before the formation of the ordered H_{II} phase (95–100% DLPE). Our current fluorescence results further agree well with the observed increase in C═O vibrational frequency at ~65% DLPE, using an independent and noninvasive Fourier transform infrared technique and the identical DLPE/POPC system with identical sample preparation (Cheng, 1994). This agreement implies that the possible tighter packing among lipids at the lipid/water interfacial region, where the carbonyl groups are located, may be partially responsible for the higher order packing of the covalently attached DPH of DPH-PC in the "intermediate" state of DLPE/POPC matrix.

The increase in curvature-associated rotational diffusion constant D_H ($= D_L/R^2$) at around 60–70% DLPE may signify either a change in the local curvature (i.e., R) of the lipid layer and/or an alteration of the lateral diffusion D_L of the lipids. Based on the independently estimated D_L, the contribution of local curvature can be delineated. Here a trend of the change in R from very large (correponding to near-zero D_H) for DLPE < 60%, to 30 Å for 70–80% DLPE and finally to 20 Å for 90–100% DLPE is clearly found. The above R "transition" ranges reflect the change of local curvature from the predicted planar L_α phase to the packing-defects-dominated D state to the curved H_{II} phase. The predicted 20-Å curvature agrees well with the direct curvature determination of H_{II} phase in PE membranes (Gruner et al., 1985). Obviously, the above crude calculations are based on the assumptions that the lateral diffusion behaviors of DPH-PC and Py_rPC are similar and that the lateral diffusion coefficients of lipids are isotropic, i.e., independent of the directions of lateral motions (Chen et al., 1990).

It is interesting to mention that the onset of all the rotational dynamics parameters is found at around 65%, which is about 10–15% less than the onset of "intermediate" state predicted by NMR (Boni and Hui, 1983). As described above, this "earlier" onset has also been found by using a noninvasive FTIR method by monitoring the behavior of C═O vibrations of the same lipid mixtures (Cheng, 1994). Our results therefore suggest that the "faster" timescale spectroscopic techniques (e.g., nanosecond fluorescence and subpicosecond vibrational IR) are able to detect the onset of packing defects much better than the milli- to microsecond averaged NMR. The sensitivity of other fluorescence probes (e.g., Laurdan) in monitoring the "onset" of packing defects has also been reported recently (Epand, 1995, and references therein).

Recently several studies (van der Meer et al., 1990; van der Sijs et al., 1993; Muller et al., 1994) have indicated that the orientational distribution of site-specific fluorophores, e.g., DPH-PC and trimethylamonium DPH (TMA-DPH), can be estimated from time-resolved fluorescence anisotropy measurements. Some studies preferred (e.g., van der Meer et al., 1990; Chen et al., 1992) the use of even-parity-only orientational potential, whereas others (e.g., van der Sijs et al., 1993; Muller et al., 1994) indicated the importance of including odd-parity terms in the orientational potential. The latter is based on the argument of the symmetry of distribution of probes on both sides (leaflets) of the lipid bilayer (Chen et al., 1992; Muller et al., 1994). In our case, the PE/PC membranes consist of bilayer (L_α) and monolayer (H_{II})-type ordered structures, as well as the mesoscopic D state, which has a combination of both structures and others. Because of the complicated and heterogeneous nature of this PE/PC membrane system, we prefer to employ simple models, one-exponential and WOBHOP, which require no prior assumptions of the parity of the orientational potential, as discussed in Materials and Methods. Furthermore, the term "existence of packing defects" used in this study refers to the presence of curvature-associated defects as revealed by the abrupt increase in D_H. Extensive fluorescence anisotropy studies (van der Sijs et al., 1993; Muller et al., 1994) of fluorescence probes in bilayer membranes have indicated that "defects" or "fluctuating voids" can also exist in bilayer membranes. We believe that the curvature-associated "packing defects" in

PE/PC membranes arise over and above those "fluctuating voids" predicted for other bilayer membranes.

In summary, the time-resolved fluorescence polarization technique as described in this study provides a useful means of exploring the rotational dynamics and orientational distribution of lipids in membranes exhibiting mesoscopic packing defect state with no long-range translational order. Based on a simple molecular dynamics model (WOBHOP), the recovered rotational diffusion parameters, D_W and D_H, of DPH-PC allow one to detect subtle changes in the rotational mobility of lipids as a result of the appearance of local curvatures of the membranes in the mesoscopic D state. The local order parameter $\langle P_2 \rangle$ of DPH-PC reflects the packing constraint imposed on the site-selective DPH and is sensitive to the "transition" involving curvatures. The application of this sensitive molecular dynamics technique to more complicated membranes, as well as other self-assembling systems, will be pursued further.

We sincerely thank Dr. Y. K. Levine for providing useful criticisms and suggesting the use of odd-parity potential function to fit the fluorescence data. We acknowledge the enlightening discussions of Dr. van der Meer regarding the possible parity and symmetry of the orientational potentials in lipid layers of different geometries.

This work was supported by grants from the National Institutes of Health (CA 47610) and the Robert A. Welch Research Foundation (D-1158) to KHC.

REFERENCES

Ameloot, M., H. Hendricks, W. Herreman, F. Van Canwelaert, and B. W. van der Meer. 1984. Effect of orientational order on the decay of the fluorescence anisotropy in membrane suspensions. Experimental verification on unilamellar vesicles and lipid/α-lactalbumin complexes. *Biophys. J.* 46:247–256.

Boni, L. T., and S. W. Hui. 1983. Polymorphic phase behavior of dilinoleoylphosphatidylethanolamine and palmitoyloleoylphosphatidylcholine mixtures. *Biochim. Biophys. Acta.* 731:177–185.

Burgess, S. W., T. J. McIntosh, and B. R. Lentz. 1992. Modulation of poly(ethylene-glycol)-induced fusion by membrane hydration: importance of interbilayer separation. *Biochemistry.* 31:2653–2661.

Chen, S.-Y., K. H. Cheng, and B. W. van der Meer. 1992. Quantitation of lateral stress in lipid layer containing non-bilayer phase preferring lipids by frequency-domain fluorescence spectroscopy. *Biochemistry.* 31: 3759–3768.

Chen, S.-Y., K. H. Cheng, B. W. van der Meer, and J. M. Beechem. 1990. Effects of lateral diffusion on the fluorescence anisotropy in hexagonal lipid phases. 2. Experimental study. *Biophys. J.* 58:1527–1537.

Cheng, K. H. 1989. Fluorescence depolarization study of lamellar liquid crystalline to inverted micellar phase transition of phosphatidylethanolamine. *Biophys. J.* 55:1025–1031.

Cheng, K. H. 1994. Infrared study of the bilayer stability behavior of binary and ternary phospholipid mixtures containing unsaturated phosphatidylethanolamine. *Chem. Phys. Lipids.* 70:43–51.

Cheng, K. H., and J. R. Lepock. 1992. Inactivation of calcium uptake by EGTA is due to an irreversible thermotropic conformational change in the calcium binding domain of the Ca-ATPase. *Biochemistry.* 31: 4074–4080.

Cheng, K. H., P. Somerharju, and I. Sugar. 1994. Detection and characterization of the onset of bilayer packing defects by nanosecond-resolved intramolecular excimer fluorescence spectroscopy. *Chem. Phys. Lipids.* 74:49–64.

Deinum, G., H. Van Langen, G. Van Ginkel, and Y. K. Levine. 1988. Molecular order and dynamics in planar lipid bilayers: effect of unsaturation and sterols. *Biochemistry.* 27:852–860.

Epand, R. M. 1995. Comments on fluorescence methods for probing local deviations from lamellar packing. *J. Fluorescence.* 5:3–8.

Galla, J.-J., W. Hartmann, U. Theilen, and E. Sackmann. 1979. On two-dimensional passive random walk in lipid bilayers, and fluid pathways in biomembranes. *J. Membr. Biol.* 48:215–236.

Gratton, E., D. M. Jameson, and R. D. Hall. 1984. Multifrequency phase and modulation fluorometry. *Annu. Rev. Biophys. Bioeng.* 13:105–124.

Gruner, S. M., P. R. Cullis, M. J. Hope, and C. P. S. Tilcock. 1985. Lipid polymorphism: the molecular basis of non-bilayer phases. *Annu. Rev. Biophys. Biophys. Chem.* 14:211–238.

Lakowicz, J. R., and B. P. Malieval. 1985. Construction and performance of a variable frequency phase modulation fluorometer. *Biophys. Chem.* 21:61–78.

Litzinger, D. C., and L. Huang. 1992. Phosphatidylethanolamine liposomes: drug delivery, gene transfer and immunodiagnostic applications. *Biochim. Biophys. Acta.* 113:201–227.

Muller, J. M., E. E. van Faassen, and G. van Ginkel. 1994. Experimental support for a novel compound motion model for the time-resolved fluorescence anisotropy decay of TMA-DPH in lipid vesicle bilayers. *Chem. Phys.* 185:393–404.

Parente, R. A., and B. R. Lentz. 1985. Advantages and limitations of 1-palmitoyl-2-[[2-[4-(6-phenyl-*trans*-1.3.5-hexatrienyl) phenyl]ethyl-]carbonyl]-3-*sn*-phosphatidylcholine as a fluorescent probe. *Biochemistry.* 25:1021–1026.

Spencer, R. D., and G. Weber. 1970. Influence of Brownian rotations and energy transfer upon the measurements of fluorescence lifetime. *J. Chem. Phys.* 52:1654–1663.

Sugar, I. P. 1991. Use of Fourier transform in the analysis of fluorescence data. 1. A general method for finding explicit relationship between photophysical models and fluorescence parameters. *J. Phys. Chem.* 95:7508–7515.

Thevenin, B. J.-M., N. Periasamy, S. B. Shohet, and A. S. Verkman. 1994. Segmental dynamics of the cytoplasmic domain of erythrocyte band 3 determined by time-resolved fluorescence anisotropy: sensitivity to pH and ligand binding. *Proc. Natl. Acad. Sci. USA.* 91:1741–1745.

van der Meer, B. W., K. H. Cheng, and S.-Y. Chen. 1990. Effects of lateral diffusion on the fluorescence anisotropy in hexagonal lipid phases. 1. Theory. *Biophys. J.* 58:1517–1526.

van der Sijs, D. A., E. E. van Faassen, and Y. K. Levine. 1993. The interpretation of fluorescence anisotropy decays of probe molecules in membrane systems. *Chem. Phys. Lett.* 216:559–565.